



LOCALIZATION OF WIND TURBINE NOISE SOURCES USING A COMPACT MICROPHONE ARRAY WITH ADVANCED BEAMFORMING ALGORITHMS

Rakesh C. Ramachandran, Hirenkumar Patel and Ganesh Raman
Fluid Dynamic Research Center, Illinois Institute of Technology
10 W 32nd St, 60616, Chicago, IL, USA.
(email: Raman@iit.edu)

Robert P. Dougherty
OptiNav Inc.
1414 127th Place NE#106, 98005, Bellevue, WA, USA.

ABSTRACT

One of the challenges that one faces when developing and designing low noise wind turbines is knowledge of components that radiate the most noise. Typical measurement techniques using a single microphone will result only in the overall sound pressure level radiated by the wind turbines. When it comes to locating sources of noise on a wind turbine, advanced techniques such as the microphone array in conjunction with beamforming algorithms are required. Earlier work has examined wind turbine noise using a microphone array with 148 microphones. These microphones were spread out on the ground over an area of 270 m^2 near the wind turbine and were not mobile and compact. This paper focuses on using a compact mobile microphone array with advanced beamforming algorithms to measure the noise radiated from wind turbines and identify them with their corresponding sources. Our initial experimental observation on locating the components on a wind turbine radiating noise suggests that it is indeed possible to locate these sources using a compact 24 microphone array with advanced beamforming algorithms such as DAMAS2, CLEAN-SC and TIDY. The qualification experiments performed on the array in laboratory using synthetic noise sources showed the differences between the various advanced beamforming algorithms. In locating the noise sources at desired narrowband frequencies CLEAN-SC was found to perform the best followed by DAMAS2 and conventional frequency domain beamforming. At desired broadband frequencies TIDY performed better in locating the source followed by delay-and-sum. It was also observed that the knowledge of Rayleigh criterion played an important role in locating the sources at the lower frequencies. The experimental results on a full scale wind turbine reveal that most noise radiated were due to aerodynamic noise from the blade tip and mechanical noise from nacelle. Additionally, we

were able to measure and locate the noise radiated due to the yaw motors in particular. The initial results presented here offer strong evidence of the potential of compact microphone arrays in measuring and locating the noise sources on wind turbines.

1 INTRODUCTION

Wind energy is emerging as a centerpiece of the new energy economy, because it is abundant, inexpensive, inexhaustible, widely distributed, and clean. The US Department of Energy's report '20% Wind Energy by 2030' envisioned that wind power could supply 20% of all U.S. electricity by the year 2030. In this new age of clean energy revolution many urban cities are considering buildings which are self sustaining when it comes to energy. A primary concern when it comes to using wind energy, especially near dwellings and urban cities, is the noise that the wind turbines radiate. Like any other machine with rotating components, wind turbines are not an exception when it comes to noise. There is great interest to design and develop low noise wind turbines. An important aspect of reducing wind turbine noise is locating the sources on the wind turbine which generate the maximum noise. Typically, wind turbine noise is measured using a single microphone (for compliance purposes) which provides us with a quantitative value of the total noise being radiated from the wind turbine. It is however impossible to map the noise level to individual sources on the wind turbine using a single microphone. In order to locate the sources on a wind turbine we would have to use a microphone array. Measuring wind turbine noise using a microphone array is not new. Oerlemans et. al. [4] in their effort to measure and localize wind turbine noise used a large microphone array with 148 microphones spread over an area of $270 m^2$. Our motivation for this work was to employ a compact and mobile array (of the order of $1.5 m^2$) to measure and effectively locate the noise sources on the wind turbine. We achieved this by using advanced beamforming algorithms (DAMAS2, CLEAN-SC and TIDY) instead of conventional methods of beamforming, such as, frequency domain beamforming (FDBF) and delay and sum (DAS).

1.1 Wind Turbine Noise

Wind turbines generate both aerodynamic and mechanical noise from its various components (see Fig. 1). Aerodynamic noise includes low-frequency sound, in-flow turbulence sound, and airfoil self- noise as explained by Wagner [8]. Mechanical sources include sound from the gearbox, generator, yaw drives, cooling fans, and hydraulics. Mechanical sounds originate from the relative motion of mechanical components and their dynamic response. Examples of mechanical sound sources include the gear box that houses gears that connect the low speed shaft to the high speed shaft. Typically the rotor blade rotations occur at 30-60 rotations per minute (rpm). These rotations are transmitted to the high speed shaft at 1000-1800 rpm and during the process noise is produced by the gears and the high speed shaft. The aerodynamic noise on the other hand is due to the blade motion in air is primarily broadband in nature (see Fig. 2). There are two mechanisms that gives rise to the aerodynamic noise, namely, (i) inflow turbulence noise and (ii) airfoil self-noise. The inflow turbulence noise is due to the interaction of turbulence in the atmosphere with the leading edge of the blades. This mechanism has been shown to emit low frequency noise (around 200 Hz). Airfoil self-noise arises when an airfoil section encounters a steady, non- turbulent flow field. The two main contributors of this noise

are the trailing edge noise and the tip vortex noise. The trailing edge noise is caused by the interaction of the turbulent boundary layer with the trailing edge of the blade. The tip vortex noise is known to contribute mostly to high-frequency broadband airfoil self-noise.

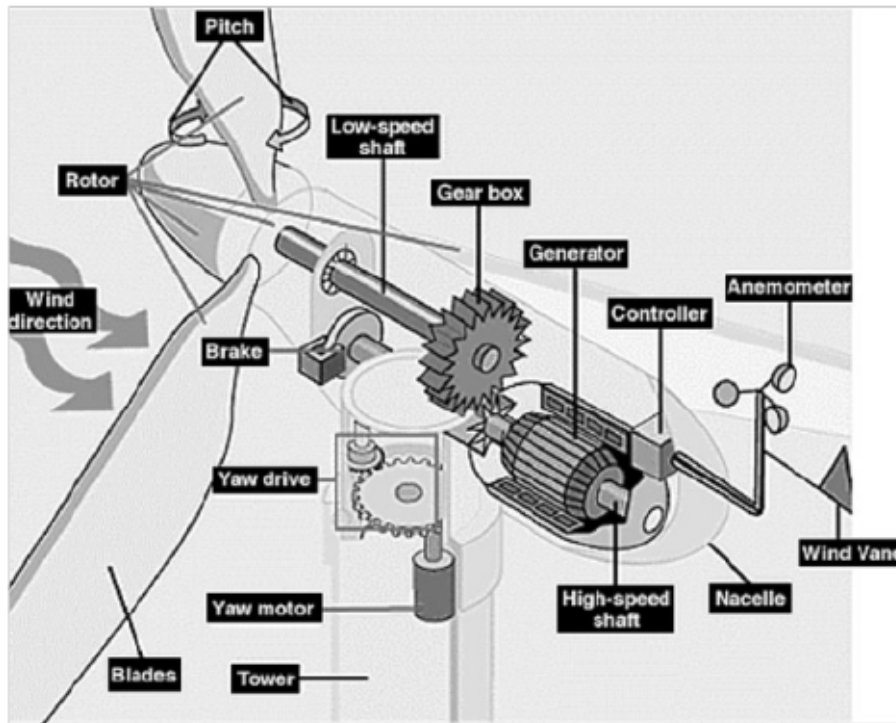


Figure 1: Components of wind turbine. [6]

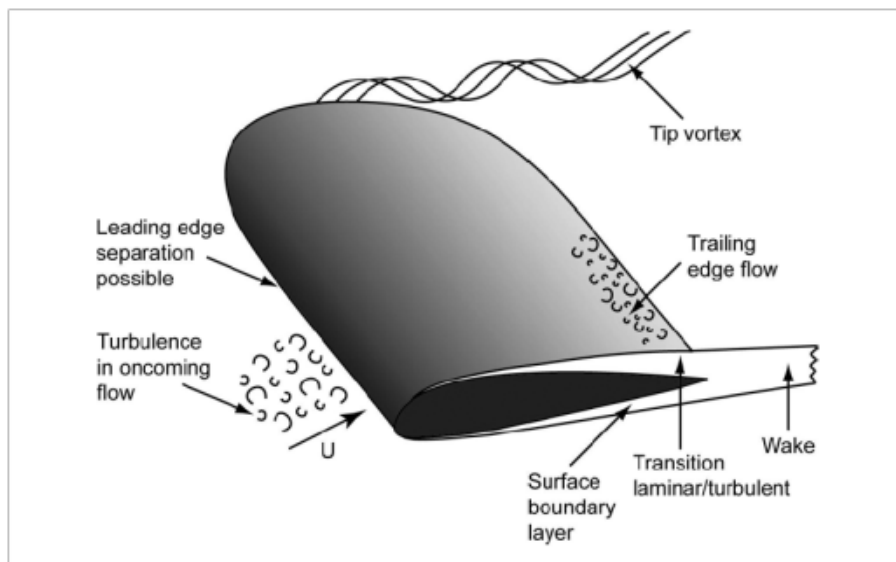


Figure 2: Noise producing mechanism on a rotor blade. [8]

1.2 Beamforming

The conventional beamforming algorithms include the frequency domain beamforming and the delay and sum beamforming. In the frequency domain beamforming the source is assumed to be a monopole source. Since the locations of the sources are unknown in practice, a scanning grid that covers a region of interest with a certain resolution is formed. Propagation vectors from each of these grid points to all the microphones in the array is calculated. Using a suitable weight factor for the propagation vectors and along with the cross spectral matrix (CSM) computed from the microphone array measurements we find a beamform map which gives us the location of the source on the scanning grid. The beamform map so formed will have poor resolution while using compact arrays. In order to get a much cleaner spectrum we have to use more advanced beamforming algorithms. The deconvolution approach for the mapping of acoustic sources (DAMAS), developed by Brooks and Humphreys [1] is one such algorithm. The basic concept behind this algorithm is that every point source on the grid will have a point spread function (psf) depending upon the resolution of the array. The beamform map hence obtained from the conventional beamforming is a result of convolution of the point source and its psf. Thus by using the psf and deconvoluting with the conventional beamform map one could obtain a much cleaner beamform map. This problem could be posed as a non-linear system of equations and solved using iterative techniques such as Gauss-Seidel method. The DAMAS algorithm however is not so efficient on the computing time as the psf have to be calculated for every iteration. This problem was overcome in DAMAS2 (DMS2), suggested by Dougherty [2], which uses a shift invariant psf instead of calculating psf every single time. The CLEAN algorithm based on spatial coherence (CLEAN-SC), developed by Sijtsma [7], is another popular advanced beamforming technique which uses the conventional beamform map as the dirty map and subtracts out the dominant source from the dirty map and iteratively builds a clean map which includes only the most dominant coherent source. Since CLEAN-SC does not use any calculated psf it is more robust. The beamforming techniques mentioned above are all narrow-band beamforming techniques. As the wind turbine noise falls in the broadband noise category we have to also make use of wideband beamforming techniques. The conventional wideband beamforming technique is the delay and sum technique. In this the time delay for the signal at every grid point to reach each microphone in the array is calculated and is subtracted off the measured signal. These subtracted signals are then summed to give the final beamform map. As before the resolution of this beamform map will be poor and in order for a cleaner map we use an advanced wideband beamforming algorithm named TIDY, developed by Dougherty [3]. It is philosophically similar to CLEAN-SC, but it works in the time domain using the cross correlation matrix (CCM) instead of the frequency domain with CSM, i.e., it uses the beamform map obtained from the DAS rather than FDBF.

2 EXPERIMENTAL SETUP

For our study we used the OptiNav Array 24 which has 24 microphones arranged in a single-arm spiral layout with the outermost sensors located at a distance of 0.72 m with a centrally located camera. The signal from the microphone array is acquired by an A/D converter which has 24 I/O audio interfaces. A MAGMA express box handles the task of interfacing the PCI 424 card to the computer. A USB cable connects the camera to a USB port on the computer. The

sound sources for the qualification experiments were produced using three 4 Ohm dual cone speaker with a maximum power of 60 W connected to a dedicated amplifier which received input from a white/tonal noise generator. The speakers were mounted on a rectangular frame support which had 21 different mounting locations each separated by distance of 2.54 cm (1 in.). For detailed description of the experimental setup please refer to [5]. A schematic of the experimental setup of synthetic sources and the microphone array used are shown in Fig. 3. The full scale wind turbine tests were made on a GE 1.5 MW wind turbine. The picture of this wind turbine is shown in Fig. 4. This wind turbine has a hub height of 85m with the rotor diameter of 77m. The turbine has a variable rotor speed of 10.1 to 20.4 rpm. The rated wind speed of this turbine is 12 m/s. The mean speed of the wind turbine during the field experiments was 12 rpm, which corresponds to Mach number of 0.14 at the blade tip. The wind turbine was also equipped with state of the art wind speed and direction detection system known as 'Catch the wind'. This system has the capability to detect wind speed and direction up to 300 m in front of the wind turbine. This system then yaws the nacelle to the detected wind direction to catch the wind. The microphone array was located at two different distances one at 85m and another at 50m from the tower. This wind had a hub height of 85m with the rotor diameter of 77m. The wind turbine is located at the Invenenergy farm at Grand Ridge, Illinois, USA.

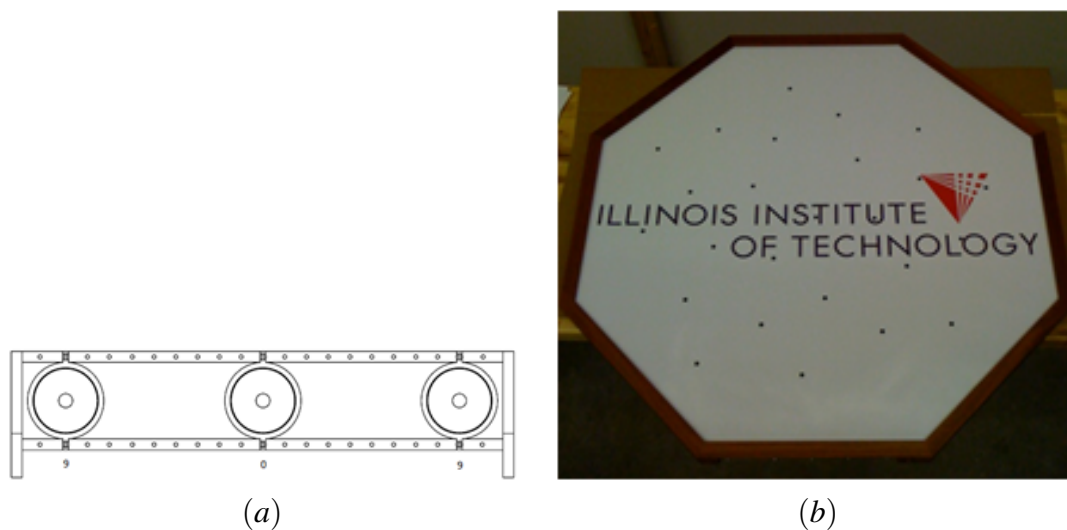


Figure 3: Schematic of: (a) speaker arranged on a rectangular frame support and, (b) the microphone array.

3 QUALIFICATION OF ARRAY

Before conducting measurements on the full scale wind turbine, we conducted several qualification experiments to study the behavior of the various beamforming algorithms when subjected to different types of noise. Detailed discussion of results of these experiments can be found in reference [5]. One of the most interesting findings from this study was that the all beamforming



Figure 4: The GE 1.5 MW wind turbine located at the Invenergy wind farm in Grand Ridge, Illinois.

algorithms were limited in locating multiple sources by the Rayleigh criterion. The Rayleigh criterion is given by Eq. 1;

$$W = \frac{rD}{\lambda z} \quad (1)$$

where, $W = 1.22$ is the Rayleigh limit which is the distance between the peak and the first zero of an ideal diffraction pattern below which multiple sources cannot be separated when using a particular type of imaging system. In the equation, r is the separation distance between the sources, D is the diameter of the array, λ is the wavelength of the source and z is the distance between the array and the source. Figure 5 shows the schematic of the comparison of source frequency and separation distance between the sources according to the Rayleigh criterion. The distance between the source and array was 0.75 m and the diameter of the array was 0.72 m. The red horizontal line indicates the case where the sources are separated by a distance of 0.1 m. The black arrow indicates the frequency below which the sources cannot be separately identified. In this case that frequency is around 4000 Hz. Figure 6 shows the beamform map of the case where the three sources are separated by a distance of 0.1 m using FDBF. Figures. 6(a) and 6(b) show the beamform maps at the frequency of 1000 Hz and 6000 Hz respectively. We observe that the beamforming algorithm is not able to separate the different sources when the frequency of interest is below 4000 Hz whereas it is able to resolve the different sources when the frequency is above 4000 Hz. Similar observation is made in the case of DMS2 as shown in Fig. 7 which shows the beamform map of the same cases using DMS2. The Rayleigh criterion is not limited only to the narrowband beamformers but to the wideband beamformers also. Figure. 8 shows the

beamform maps of the case where the three sources are separated by a distance of 0.1 m using DAS. Figures. 8(a) and 8(b) show the beamform maps at the frequency range of 972.5-3445.2 Hz and 3445.2-10282.9 Hz respectively. We observe that the DAS beamformer is not able to resolve the different sources at frequencies less than 4000 Hz whereas it resolves the sources when the frequencies are greater than 4000 Hz. The same is observed in case of TIDY. Figure. 9 shows the beamform map obtained using TIDY for the same cases. From these above results we also observe that the advanced algorithms give a much cleaner map than the conventional beamformers. Figure. 10 shows the beamform map of three sources separated by a distance of 0.23 m (9 in.) using FDBF, DMS2, CLSC and TIDY for the coherent and incoherent cases. In this particular analysis the frequency band of interest was chosen to be 2292.3-2431.5 Hz and the dynamic range was chosen to be 10 dB. We observed that the FDBF, DMS2 and TIDY algorithms whose formulation was based on incoherent sources was able to pick up both the sources in both incoherent and coherent cases. The CLSC algorithm is formulated to pick out the highest of the coherent sources as evident from our results. Also in the incoherent case the CLSC was able to locate both the sources.

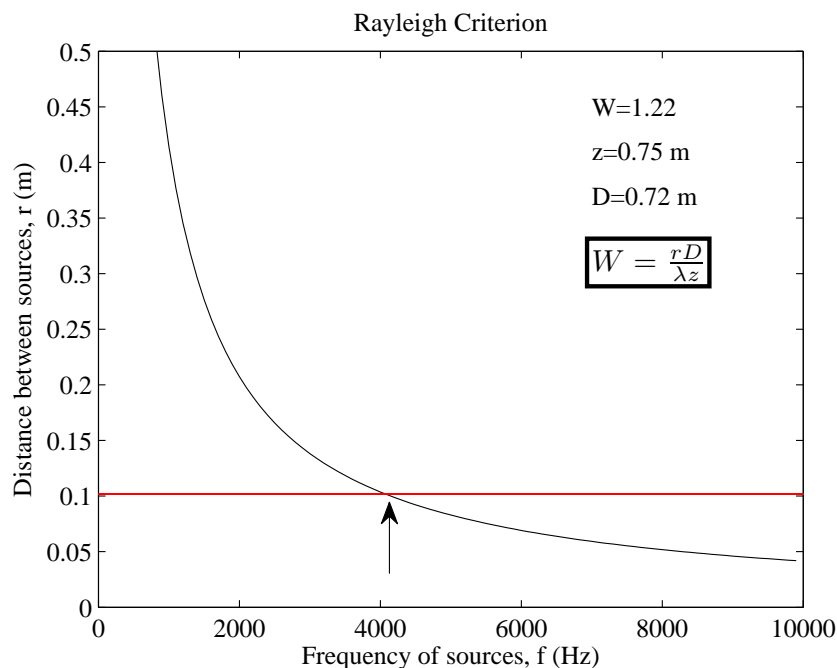


Figure 5: Separation distance between the sources against frequency of signal calculated using Rayleigh criterion.

4 WIND TURBINE NOISE SOURCES

Measurements on the wind turbine at the wind farm were conducted with a wind screen (polyurethane foam) placed on top of the microphone array to avoid any additional noise at the microphone due to interaction with wind. In order to account for the loss in amplitude due to the wind screen a calibration was performed using a blow horn at the foot of the tower.

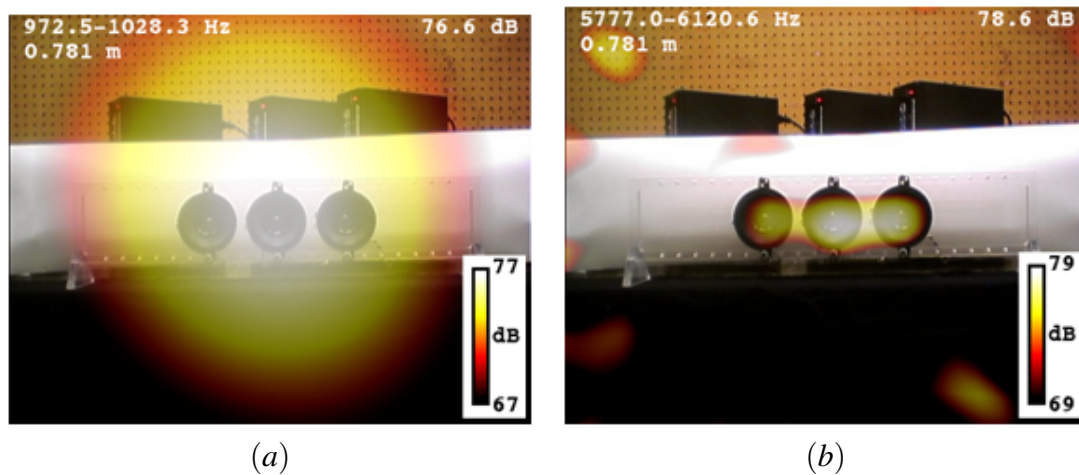


Figure 6: Beamform map of three sources separated by a distance of 0.1 m (4 in.) using FDBF at frequency ranges of; (a) 972.5-1028.3 Hz, and (b) 5777-6120.6 Hz.

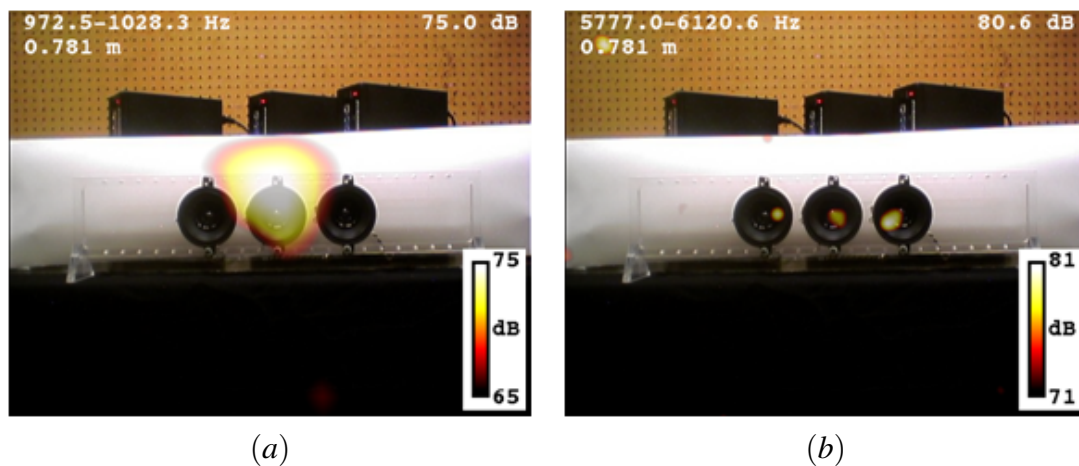


Figure 7: Beamform map of three sources separated by a distance of 0.1 m (4 in.) using DMS2 at frequency ranges of; (a) 972.5-1028.3 Hz, and (b) 5777-6120.6 Hz.

A pre-calibrated 6.35 mm B&K microphone was used as the reference microphone. A comparison of the spectrum obtained from both the B&K microphone and the array is shown in Fig. 11(a). From this figure a mean difference of 10 dB was observed between both the spectra. The beamform map of the calibration test using CLSC is shown in Fig.11(b).

Figure. 12 shows the beamform map of the wind turbine noise using DAS and TIDY. We observe that the map from basic beamforming does not separate any sources on the wind turbine. The advanced beamforming algorithm (TIDY) separates the nacelle noise from the aerodynamic blade noise. The nacelle noise is believed to be due to the various mechanical components inside the nacelle, such as, gearbox, cooling fans, etc. The aerodynamic noise is believed to be trailing edge noise and blade tip noise as observed by Oerlemans [4] in his work. Figure. 13 shows the

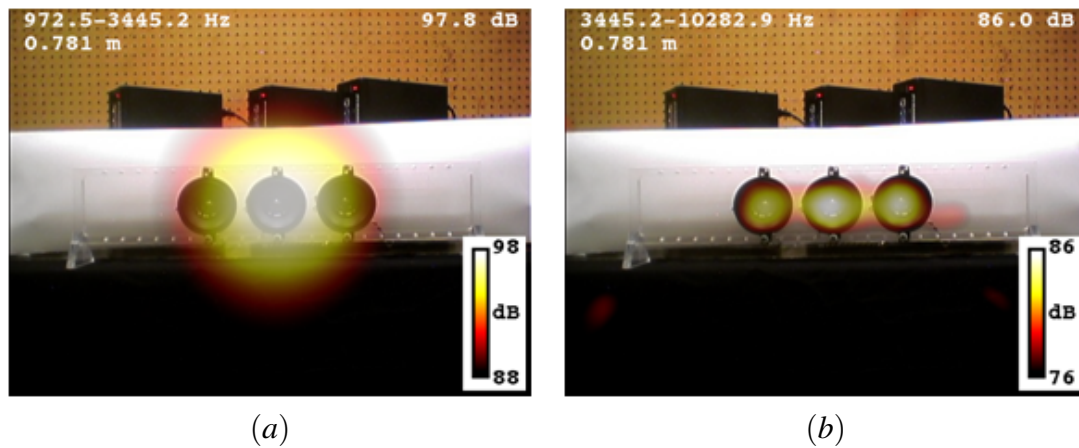


Figure 8: Beamform map of three sources separated by a distance of 0.1 m (4 in.) using DAS at frequency ranges of; (a) 972.5-3445.2 Hz, and (b) 3445.2-10282.9 Hz.

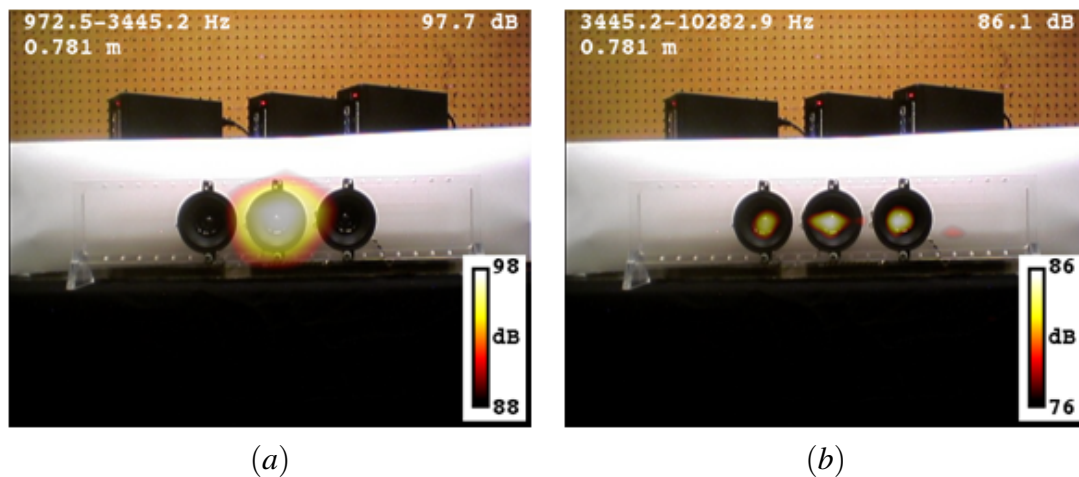


Figure 9: Beamform map of three sources separated by a distance of 0.1 m (4 in.) using TIDY at frequency ranges of; (a) 972.5-3445.2 Hz, and (b) 3445.2-10282.9 Hz.

beamform map of the blade noise alone using the TIDY algorithm. The blades were rotating in counter-clockwise direction in this case. The immediate observation from this beamform map is the striking asymmetry, i.e., more noise seems to be produced during the downward motion of the blades (when the observer is on the ground). This is attributed to the convective amplification and directivity of the trailing edge noise as explained by Oerlemans [4].

One of the major advantages of using the microphone array is the ability to separate individual noise sources from the overall sound measured. A prime example for such application is discussed here. When there is a change in wind direction detected by the system, the yaw motors are activated to turn the nacelle to the direction in which the wind blows. Figure. 14 shows wind direction and speed data obtained by the system over a period of 60 sec. In this,

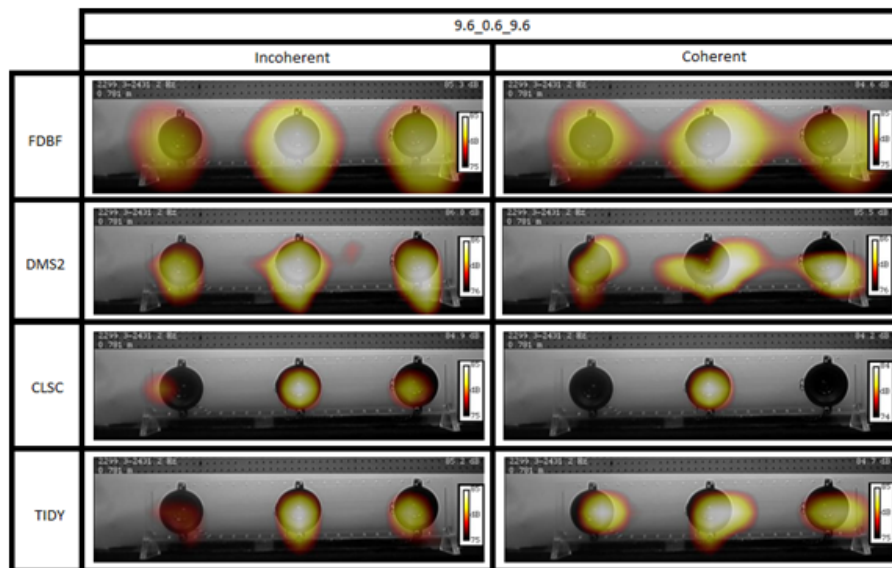


Figure 10: Comparison of beamform maps obtained from FDBF, DMS2, CLSC and TIDY for three incoherent and coherent sources of the same amplitude.

we observe that the system detects the change in wind speed and direction at about 30 sec. The microphone array was used to measure the noise emitted during the same 60 sec period. Figure. 15 shows the frequency spectrum obtained from the microphone array during this time period. We clearly observe that the yaw motor operation radiates a tonal noise of around 1100 Hz starting at about 30 sec. Figure. 16 shows the beamform map of the noise radiated by yaw motor using CLSC before and after it was turned on. We observe that there is an increase of around 20 dB when the yaw motors were operating.

5 SUMMARY

The results of the initial qualification experiments of the array provided us with the knowledge of how various beamforming algorithms behave on exposure to different types on noise sources. The FDBF, DMS2 and CLSC were all limited to narrowband analysis where as DAS and TIDY could be used for broadband analysis. Even though the FDBF, DMS2 and TIDY beamformers were all formulated on the assumption of incoherent sources, they were able to locate coherent sources as well. The CLSC beamformer was formulated to pick the maximum of the coherent sources as evident from our experimental results. The CLSC however was able to locate the incoherent sources too. In terms of the frequency of the source, for the particular array and the distance of the source from the array, the microphone array was able to clearly locate the sources above 1000 Hz using all the algorithms. From the qualification study it was clear that there was no single algorithm that was perfect for measuring wind turbine noise. In order to study the narrow band sources CLSC was found to be the best algorithm and for broadband analysis TIDY was the best. From the results of full scale wind turbine measurements, it was evident that the compact microphone array was effectively able to separate various noise sources, both mechanical and aerodynamic, produced by the wind turbine. The asymmetry in

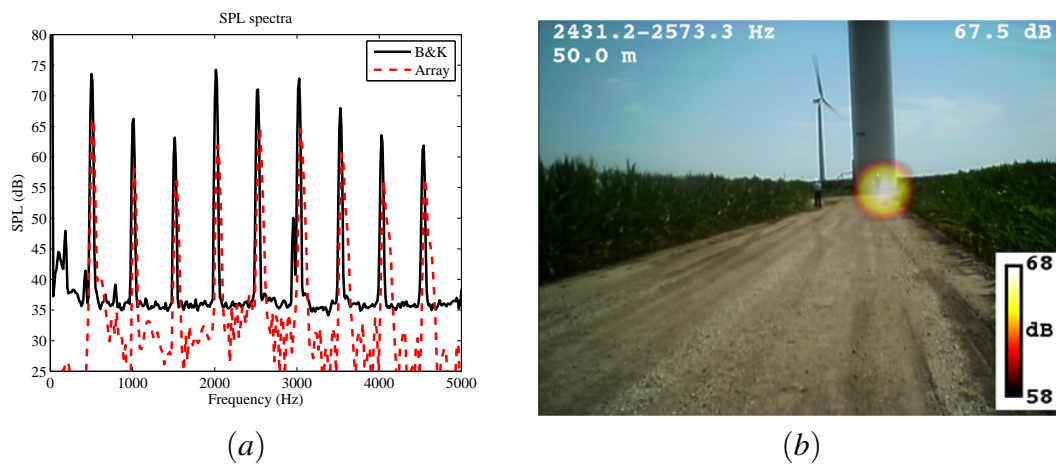


Figure 11: Calibration experiment data; (a) Comparison of frequency spectrum obtained from B&K microphone and the microphone array, and (b) Beamform map of the calibration source obtained using CLSC.

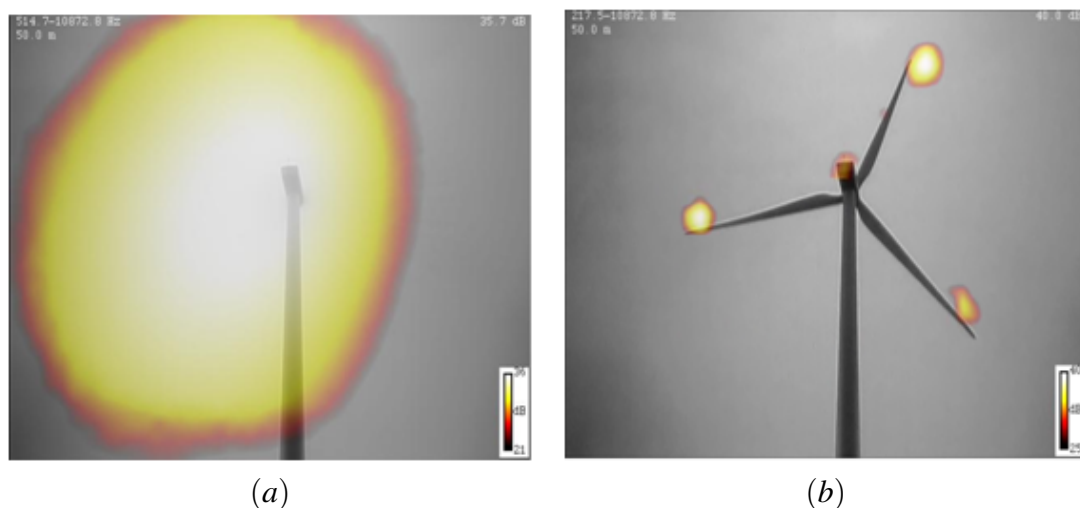


Figure 12: Beamform map of a 1.5 MW wind turbine using; (a) DAS beamformer, and (b) TIDY beamformer.

the aerodynamic noise was attributed to convective amplification and directivity of the trailing edge noise. These results obtained using a compact and mobile microphone array in conjunction with advanced beamforming algorithms are in good agreement with those reported in the work of Oerlemans et. al. [4] conducted using a very large array. Further we were able to separate out the yaw motor noise from the noise emitted by other mechanical components inside the nacelle. This demonstrates the potential of the compact and mobile microphone arrays as a valuable tool for industries to design and develop low noise wind turbines and also for monitoring the noise emitted by different components of wind turbine for maintenance.

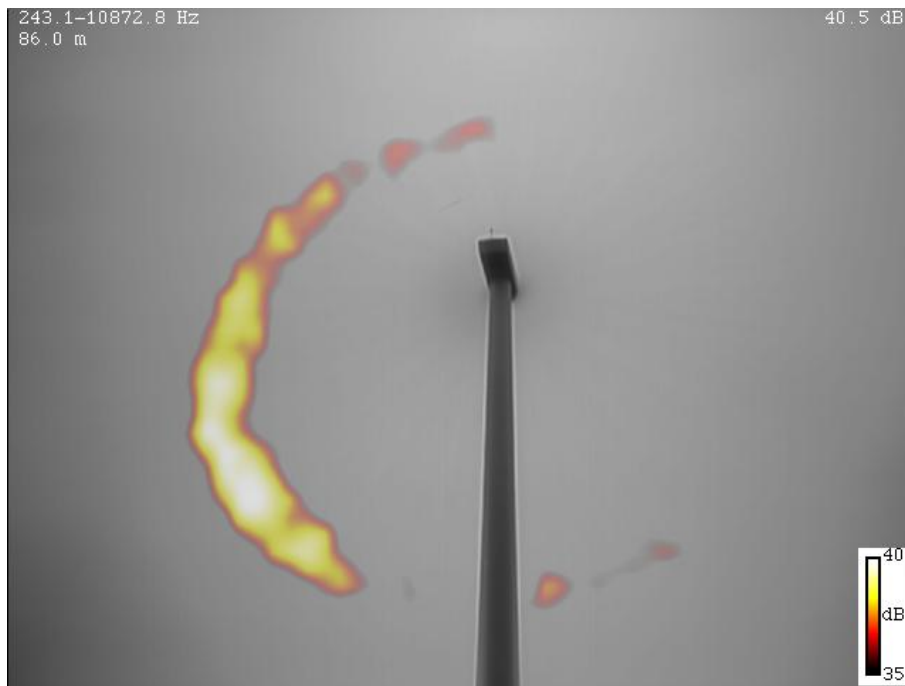


Figure 13: Beamform map of the aerodynamic noise produced at the blade trailing edge using the TIDY beamformer.

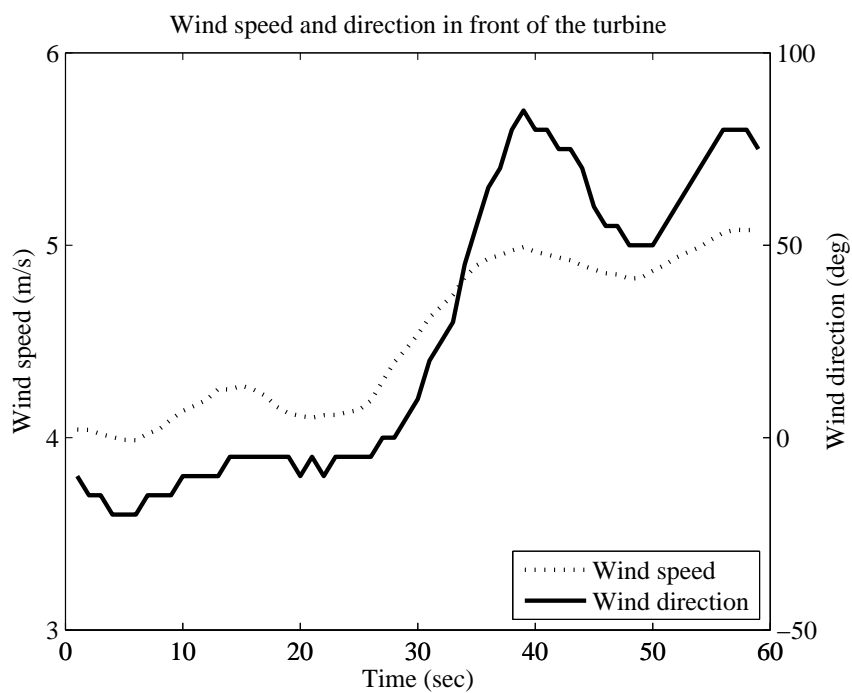


Figure 14: Wind speed and wind direction data measured in front of the turbine over a period of 60 sec obtained from 'Catch the wind' system.

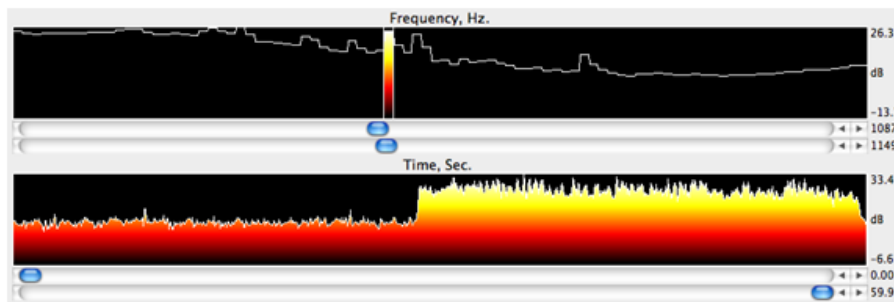


Figure 15: Frequency spectrum and time series from the microphone array showing the noise component from the yaw motors.

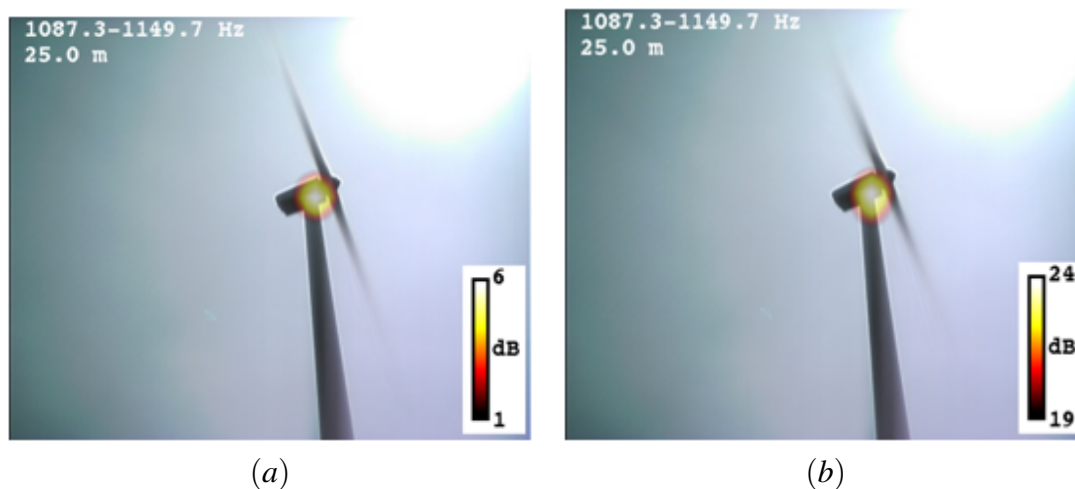


Figure 16: Beamform map of a 1.5 MW wind turbine using CLSC; (a) when the yaw motors are not operational, and (b) when the yaw motors are operational.

6 ACKNOWLEDGEMENTS

This work was funded by the U.S. Department of Energy with Mr. Brian Conner as program manager. The authors are also grateful to Mr. Charles Murray and Mr. Jacob Ursua of Invenergy wind farm, Grand Ridge, IL, USA for their assistance with arrangements for measurements made at the wind farm.

REFERENCES

- [1] T. F. Brooks and W. M. Humphreys, Jr. “A Deconvolution Approach for the Mapping of Acoustic Sources (DAMAS) determined from phased microphone array.” *J. Sound Vib.*, 294(4-5), 856–879, 2006.
- [2] R. P. Dougherty. “Extensions of DAMAS and Benefits and Limitations of Deconvolution

- in Beamforming.” AIAA-2005-2961, 2005. 11th AIAA/CEAS Aeroacoustics Conference, Monterey, California, May 23-25, 2005.
- [3] R. P. Dougherty and G. Podboy. “Improved Phased Array Imaging of a Model Jet.” AIAA-2009-3186, 2009. 15th AIAA/CEAS Aeroacoustics Conference (30th AIAA Aeroacoustics Conference), 11 - 13 May 2009, Miami, FL.
- [4] S. Oerlemans, P. Sijtsma, and B. Méndez López. “Location and Quantification of Noise Sources on a Wind Turbine.” *J. Sound Vib.*, 299, 869–883, 2007.
- [5] R. C. Ramachandran and G. Raman. “Evaluation of Various Beamforming Algorithms for Wind Turbine Noise Measurement.” AIAA-2011-2388, 2011. 49th AIAA Aerospace Sciences Meeting, 4-7 January 2011, Orlando, FL.
- [6] G. Raman. “Wind Turbines: Clean, Renewable and Quiet?” *Noise & Vibration Worldwide*, 40, 15–21, 2009.
- [7] P. Sijtsma. “CLEAN Based on Spatial Source Coherence.” *Int. J. Aeroacoustics*, 6, 357–374, 2007.
- [8] S. Wagner, R. Bareib, and G. Guidati. *Wind Turbine Noise*. Springer, Berlin, 1996.